Title:

Future CO_2 fertilization of the Amazon forest hinges on plant phosphorus use and acquisition

Author list:

K. Fleischer*, *Land Surface–Atmosphere Interactions, Technical University of Munich, Germany*
A. Rammig, *Land Surface–Atmosphere Interactions, Technical University of Munich, Germany*
M. G. De Kauwe, *University of New South Wales, Australia*
A.P. Walker, *Oak Ridge National Laboratory, United States*
T. F. Domingues, *University of São Paulo, Brazil*
L. Fuchslueger, *University of Antwerp, Belgium*
S. Garcia, *National Institute of Amazonian Research, Brazil*
D. Goll, *LSCE, France*
A. Grandis, *University of São Paulo, Brazil*
M. Jiang, *Western Sydney University, Australia*
V. Haverd, *CSIRO, Australia*
F. Hofhansl, *International Institute for Applied Systems Analysis, Austria*
J. Holm, *Lawrence Berkeley National Laboratory, United States*
B. Kruijt, *Alterra Wageningen, The Netherlands*
F. Leung, *Exeter University, United Kingdom*
B. E. Medlyn, *Western Sydney University, Australia*
L. M. Mercado, *Exeter University, United Kingdom*
R. J. Norby, *Oak Ridge National Laboratory, United States*
B. Pak, *CSIRO, Australia*
C.A. Quesada, *National Institute of Amazonian Research, Brazil*
C. von Randow, *National Institute for Space Research, Brazil*
K. J. Schaap, *National Institute of Amazonian Research, Brazil*
O. J. Valverde-Barrantes, *Florida International University, United States*
Y-P. Wang, *CSIRO, Australia*
X. Yang, *Oak Ridge National Laboratory, United States*
S. Zaehle, *Max-Planck Institute for Biogeochemistry, Germany*
Q. Zhu, *Lawrence Berkeley National Laboratory, United States*
D. M. Lapola, *University of Campinas, Brazil*
*corresponding author

Global terrestrial models currently predict that the Amazon rainforest will continue to act as a carbon sink in the future primarily due to the rising atmospheric carbon dioxide (CO_2) concentration, effectively enhancing its resilience and slowing the pace of climate change. Soil phosphorus impoverishment in parts of the Amazon basin limits biomass growth, but the role of phosphorus availability in limiting its future carbon uptake has not been considered in global model ensembles, e.g., during the Coupled Model Intercomparison Project for the 5th Assessment Report of the United Nations Intergovernmental Panel on Climate Change. Here, we simulate a planned free-air CO_2 enrichment experiment in the Amazon with an ensemble of 14 terrestrial ecosystem models. We show that phosphorus feedbacks reduce the CO_2-induced biomass carbon sink to 79 ± 63 g C m^{-2} yr^{-1} over 15 years, a reduction of ~50% compared to estimates from carbon and carbon-nitrogen models. Our results suggest that the region's resilience to climate change may be much smaller than previously assumed. Variation in the biomass C response among the phosphorus-enabled models is considerable, ranging from 5 to 140 g C m^{-2} yr^{-1}, due to contrasting assumptions relating to the flexibility in plant phosphorus use and acquisition strategies. The model ensemble involuntarily represents diverse plant functional strategies and generates a series of testable hypotheses. Experimental design need to be targeted to reduce the uncertainties around the phosphorus feedback on the CO_2 fertilization effect.

The intact Amazon rainforest acts as a substantial carbon (C) sink, completely offsetting carbon dioxide (CO_2) emissions from fossil fuel combustion and land use change in the Amazon region[1,2]. Increasing atmospheric CO_2 concentrations from anthropogenic activity may be the primary driving force for the current Amazon net carbon sink[1,3], and global models assume that this CO_2 fertilization effect will continue to provide this globally significant ecosystem service into the future[4–6]. The stimulatory effect of elevated carbon dioxide (eCO_2) on photosynthesis

and tree growth has been observed experimentally in greenhouses and in the field in open top chamber and free-air CO_2 enrichment (FACE) experiments. To date, whole-ecosystem-scale experiments (i.e., FACE) have mainly been conducted in the temperate zone and never in the tropics[7,8]. In these experiments, the eCO_2-induced increase in C uptake is generally low when other factors, such as soil nitrogen (N), are limiting[9,10].

Over large parts of the Amazon and the tropics worldwide, phosphorus (P), not N, is assumed to be the key limiting nutrient, as most P has been lost or occluded from plant uptake during millions of years of soil pedogenesis[11,12]. Forests growing on these highly weathered old soils may nonetheless be highly productive due to the evolution of multiple strategies for P acquisition and use, enabling tight cycling of P between plants and soils[13,14]. Despite this knowledge, quantifying the control of P on plant physiology, growth, and plant-soil interactions in global models, and hence its role in the forests' response to eCO_2, remains challenging[15]. This challenge is exacerbated by the scarcity of observations and distinctive species responses in hyperdiverse tropical forests[16].

Here, we study the potential interactions between eCO_2 and nutrient (N and P) feedbacks in a mature Amazonian rainforest by simulating the planned AmazonFACE experiment (+200 ppm; http://amazon-face.org/) with an ensemble of ecosystem models (n = 14, Extended Data Table 3), including three C, five carbon-nitrogen (CN), and six carbon-nitrogen-phosphorus (CNP) models[17–22]. The AmazonFACE experiment is located in a well-studied, highly productive tropical forest in Central Amazonia[23,24], growing on a strongly weathered *terra firme* Ferralsol. This ecosystem represents the low end of the plant-available P spectrum in the Amazon, consistent with ~32% of the Amazon rainforest's cover fraction[25]. *In situ* measurements were used to parameterise the models and to evaluate simulated ambient conditions (Extended Data Table 1, 2). Our aim was to generate *a priori* model-based hypotheses to highlight the state-of-the-knowledge and guide measurement strategies for AmazonFACE and other ecosystem

manipulation experiments to gain crucial process understanding of P control on the CO_2 fertilization effect.

Simulated eCO_2 (+200 ppm) had a positive effect on plant biomass C across all models but was weakest in the CNP models (Fig. 1a). The eCO_2 conditions induced average biomass C gains of 163 ± 65, 145 ± 83, and 79 ± 63 g C m^{-2} yr^{-1} after 15 years in the C, CN and CNP models, respectively (Fig. 1a). Limitations by P thus reduced the predicted biomass C sink by 52% and 46% compared to that in the C and CN models, respectively, with considerable variation across and within model groups (Extended Data Fig. 1). Plot inventories at the AmazonFACE site during the 2000s indicate an ambient aboveground biomass sink of 23 g C m^2 yr^{-1}, with an Amazon-wide[1] estimate of 64 g C m^2 yr^{-1}. The model ensemble represents ambient conditions, such as productivity and LAI, reasonably well but the set of models does diverge on some ecosystem characteristics, such as ambient biomass C increases, which range from 5 to 114 g C m^2 yr^{-1} (see more discussion on ambient model performance in Extended Data Fig. 2).

Gross and net primary productivity (GPP and NPP, respectively) are both stimulated by eCO_2 in all models, both initially (after 1 year of eCO_2) and at the end of the simulation. The CNP models show the strongest decline over the 15-year period from the initial response due to P limitation (Fig. 1b, c). The final response of NPP to eCO_2 was a 35%, 29%, and 9% stimulation for the C, CN and CNP models, respectively. In general, in the CN and CNP models, nutrient limitation is defined as nutrient demand being greater than nutrient supply. But models differ in their assumptions on how nutrient limitation controls productivity and C allocation in response to eCO_2, so that divergent responses on plant carbon use efficiency (CUE = NPP / GPP) are simulated (Extended Data Table 3). In some CN models, CUE increases because N limitation is hypothesized to reduce autotrophic respiration (Ra) via lower tissue N content. In contrast, some CNP models (e.g., CABLE and ELM-ECA) assume a direct downregulation of growth or growth efficiency (i.e., NPP) but only a small reduction in GPP, and hence the plant

CUE decreases under nutrient limitation (Extended Data Fig. 3). Elevated CO_2 induced higher fine root investments of NPP in some CN and CNP models to aid nutrient acquisition (Fig. 1c; Extended Data Fig. 4). Predicted changes in allocation with eCO_2 cause a general increase in biomass C turnover across all but one of models, partially offsetting the positive biomass C response (Extended Data Table 4). Changes in turnover largely control the long-term future CO_2 effect on the biomass C sink[26,27].

Plant growth under eCO_2 is lowest in CNP models as the low availability of soil labile P restricts P uptake either immediately (CABLE, ELM-ECA, GDAY) or over time (CABLE-POP, ELM-CTC, ORCHIDEE) (Extended Data Fig. 5). We considered the modelled P limitation on plant growth to be realistic, as the models and observations agree on soil labile P being very low (Extended Data Fig. 2). Other observations support the fact that P is extremely critical for plant productivity, such as high leaf N:P ratios of 37 and high plant P resorption (before litter fall) of 78% (Extended Data Table 1). P limitation consistently reduces the eCO_2-induced biomass C sink, but there is significant variation among CNP models due to contrasting process representations (Fig. 2; Extended Data Table 3).

P shortages downregulate growth (i.e., NPP) in all models, either directly, via photosynthesis, or via a combination of both processes. No model considers P effects on Ra. The major differences among the models relate to how they modify P supply and demand to alleviate plant P shortages, including either (i) enhancing plant P use efficiency (PUE = NPP / P uptake) or (ii) upregulating P acquisition mechanisms. PUE may change if tissue nutrient ratios are flexible, if C allocation changes among tissues with different stoichiometry, and/or if P resorption is variable. Flexible stoichiometry is considered in all CNP models except ELM-CTC, although with varying degrees of flexibility, such that the stoichiometry in CABLE and ORCHIDEE is effectively fixed (Fig. 2). Greater fine root C allocation in response to plant P stress is

134 considered in ELM-ECA, GDAY and ORCHIDEE, and P resorption is a fixed fraction of leaf
135 tissue P in all models (Fig. 2).

136 In regards to modelled soil P acquisition mechanisms; three of the six models (ELM-ECA,
137 ELM-CTC, GDAY) consider desorption of P from mineral surfaces (i.e., the secondary or
138 strongly sorbed P pool), whereas the others assume P in those pools to be unavailable to plants.
139 All the models include biochemical mineralization of organic P via phosphatase, but only three
140 (ELM-ECA, ELM-CTC and ORCHIDEE) include the functionality to increase P acquisition
141 via this mechanism under plant P stress (Fig. 2; Extended Data Table 3). Litter and soil
142 stoichiometry are considered with varying degrees of flexibility. Soil labile P limits microbial
143 decomposition rates of litter and soil, so that decomposition is reduced when immobilization
144 demands for P exceed soil labile P availability (Fig. 2; Extended Data Table 3).

145 Diverging depictions of plant P use and acquisition among the CNP models cause predictions
146 of the eCO_2-induced biomass C sink to range from 5 g C m^{-2} yr^{-1} in CABLE to 140 g C m^{-2} yr^{-1}
147 in ORCHIDEE (Fig. 3a; Extended Data Fig. 1). Greater plant PUE occurred in four of the
148 models, GDAY, ELM-ECA, CABLE-POP, and ORCHIDEE, for which shifts in tissue C:N and
149 N:P due to eCO_2 led to increases in biomass C:P ranging from ~200 to 1600 g C g P^{-1} (Fig. 3c).
150 Higher fine root investment with eCO_2, at the expense of less "P-costly" wood, offset some
151 increases in PUE in ELM-ECA and GDAY. Although higher fine root allocation was simulated
152 temporarily in ORCHIDEE (Extended Data Fig. 4), investment in wood increased over the full
153 simulation period, as was also the case in CABLE-POP (Fig. 3b).

154 Flexible biomass stoichiometry altered decomposition dynamics and induced progressive P
155 limitation in response to eCO_2, i.e., litter stoichiometry shifted towards lower quality (less N
156 and P in relation to C), reducing net P mineralization rates from microbial decomposition,
157 causing P to become increasingly unavailable to plants and accumulating in soil organic matter
158 (Fig. 3d, e). Consequently, ecosystem P retention increased marginally in some models as P

leaching rates decreased. This plant-soil-microbial feedback slowed the cycling of P in the ecosystem and exacerbated the initial P limitation (see Ref. [28] for a similar feedback during pedogenesis).

Enhanced plant P acquisition under eCO_2 effectively alleviated P limitation in two CNP models (ELM-CTC and ELM-ECA). In both, eCO_2 increased the liberation of P from the secondary pool, as higher plant P demand and uptake diminished the labile P pool, in turn causing higher desorption rates. P desorption is thus only indirectly, and not mechanistically, enhanced by plants in these models. Biochemical mineralization of P under eCO_2 responded positively in both of the models, but added only notably to additional P acquisition in ELM-CTC (Fig. 3e). Although three CNP models simulated higher fine root investments (ELM-ECA, GDAY, and ORCHIDEE), the actual P uptake return per fine root increment was marginal or came only into effect in the long-term (Extended Data Fig. 6).

In summary, the model ensemble encapsulates a range of plausible hypotheses and represents a potential range of biomass C responses to eCO_2 under low soil P availability. At the one end, CABLE assumes no plant-enabled mechanisms to acquire more P and a limited capacity for plants to use P more efficiently, resulting in effectively zero biomass C gain with eCO_2. The remaining models predicted some biomass C gain with eCO_2. Flexible stoichiometry was the key mechanistic response to eCO_2 in four of these models. ELM-CTC had no change in stoichiometry, but nonetheless predicted an increase in biomass C gain under eCO_2 based on an increase in plant P acquisition because of enhanced P mineralization and desorption.

Our results also indicate the control of N availability on modelled plant growth. The CN models simulate increased nitrogen use efficiency (NUE) and biomass C:N ratios, as N uptake was not sufficient under eCO_2 (Extended Data Fig. 5). Direct N limitation of plant growth is, however, not expected, as observations document ample N cycling in the system, e.g., high leaf N contents, indicative $\delta^{15}N$ values, high rates of N oxide emissions, and low N retention[29,30]. Plant

N availability may be underestimated in the models, since the plant-available mineral N supply was <7 g N m^{-2} across all models, as opposed to 17.5 g N m^{-2} observed in the top 10 cm only (Extended Data Fig. 2). These results highlight an important gap in our knowledge related to the dynamics of N availability, and its potential interaction with P dynamics. Future experiments should help reduce the uncertainty surrounding N effects on P limitation, in particular for regions predominantly or co-limited by N.

Divergences in the simulated eCO_2 response lead us to the following testable hypotheses:

H1. Low soil P availability will strongly constrain future plant biomass growth response to eCO_2 either by downregulating photosynthesis or limiting plant growth directly, or a combination thereof.

H2. Despite the limited soil P supply, plasticity in vegetation stoichiometry and allocation patterns will allow for some biomass growth under eCO_2.

H3. Plants will increase investments in P acquisition to increase P supply and allow biomass growth under eCO_2 either via greater P interception through fine root production or via greater P liberation from P desorption or biochemical mineralization of P.

These process- and model-based hypotheses deepen a previously carried out accounting analysis of potential N and P limitation[31]. Furthermore, we add to a model intercomparison carried out in advance of the EucFACE experiment[32] by extending the range of plant P feedbacks considered across CNP models. This work highlighted H1: two stoichiometrically constrained CNP models predicted that strong P limitation will curtail the growth response to eCO_2 in subtropical Australia. Consistent with this hypothesis, aboveground growth has not increased with eCO_2 in that experiment over the initial years[33]. This finding underlines that monitoring efforts need to place a strong(er) focus on belowground carbon allocation and soil nutrient dynamics. Additionally, the model ensemble does not yet consider the P effect on Ra

and respiration under different degrees of nutrient limitation need further monitoring during experiments to further elucidate P effects on the plant C budget and address H1.

Nutrient fertilization experiments support H2, as plasticity in leaf stoichiometry at the individual level, along with plasticity in P resorption efficiency, was observed[34]. Across the Amazon, leaf nutrient assessments indicate a leaf N:P range of 13 to 42 (n = 64) (Ref. [30]), which place our site, with a community mean ratio of 37, at the high end. GDAY thus predicted the most plausible increase in the leaf N:P ratio from 34 to 38 (Extended Data Fig. 7). CABLE-POP and ELM-ECA predicted strong increases in the leaf N:P ratio with eCO_2 but started off with much lower initial values. The degree to which plasticity in stoichiometry and resorption can aid plant PUE in highly P-limited sites that are already at the end of the observed spectrum remains to be seen (H2). Monitoring plant tissue and fresh litter nutrient content in CO_2 and nutrient fertilization experiments will give an indication of the plasticity of these plant use mechanisms in response to eCO_2.

Based on previous observations[10], a number of models assume increased fine root investment, as well as higher biochemical P mineralization and P desorption from mineral surfaces, under eCO_2-induced nutrient limitation (H3). The effect of increased fine root biomass on nutrient uptake was limited in our simulations and ambient fine root allocation fractions were highly variable among the models, ranging from 5-30% of NPP (Extended Data Fig. 4, 6). Both these modelled results highlight model deficiencies in belowground processes[35]. There is evidence that phosphatase activity in litter and soil and the presence of low-molecular-weight acids used to liberate P from organic matter or from mineral surfaces increase with plant P demand[36]. This was predicted by ELM-CTC in our simulations, which also showed Amazon-wide that "[with] enhanced phosphatase production, productivity in the highly P-limited areas can be sustained under elevated CO_2 conditions"[37]. Plants invest in P liberation and acquisition, but if these mechanisms can be upregulated under eCO_2 and over what time frame this may occur remain

233 open questions. Quantification of such fluxes is lacking, as are estimates of the associated plant
234 C costs to acquire P via these and other mechanisms, such as mycorrhizal symbiosis[14,38]. The P
235 gain and C cost for P acquisition mechanisms, as well as the associated plant-soil-microbial
236 interactions, need to be assessed by analyses of soil, microbial and root nutrition, and via novel
237 techniques investigating enzyme and labile C dynamics. Monitoring of belowground fine root
238 dynamics needs to include fine root activity in surface litter, a common phenomenon in P-
239 impoverished ecosystems in the Amazon, not yet quantified nor considered in models.

240 Previous model projections suggest a sustained fertilization effect of CO_2 on the Amazon C
241 sink but have not considered feedbacks from low soil P availability[4,5]. Our study demonstrates
242 that, based on the current generation of CNP models, the omission of P feedbacks is highly
243 likely to cause an overestimation of the Amazon rainforest's capacity to sequester atmospheric
244 CO_2. Considering P limitation on the CO_2 fertilization effect in future predictions may indicate
245 that the forest is less resilient to higher temperatures and changing rainfall patterns than
246 previously thought[4,39]. Periods of water deficit may contribute to the eCO_2 fertilization effect
247 on productivity due to its water saving effect[32]. Our study site experienced years with
248 significantly less than average precipitation, e.g. in 2000 and 2009, however, in our simulations
249 this added marginally to the modelled CO_2 effect (Extended Data Figure 8 and 9). Models are
250 not yet very apt to simulate water deficits and their consequences on plant growth and mortality
251 in general, and even more so when precipitation totals are that high[40]. Interactions of water and
252 P availability and their consequences on the CO_2 fertilization effect remain uncertain and need
253 urgent clarification[41].

254 Although P is likely to reduce the biomass C sink response to CO_2 in regions with low plant-
255 available P supply, our results suggest that plasticity in plant P use and plant P acquisition
256 mechanisms, may enable CO_2 fertilization of biomass growth. The model ensemble may be
257 interpreted as involuntarily representing a range of possible tropical plant functional strategies

and growth responses to low phosphorus availability. Responses to eCO_2 are expected to be species-specific, as were plant growth responses to low P supplies in another tropical region[16]. The ecosystem-scale response to P limitation under eCO_2 will thus depend on the relative contributions of the various P acquisition and P use strategies across individuals, their interactions and to what extent these processes can be upregulated under eCO_2. All of which ultimately need to be described and represented in a single model framework in order to accurately predict the Amazon rainforest's response to future climate change.

AmazonFACE has the unique opportunity to experimentally address these key areas of uncertainty, not only by integrating the proposed measurements across seasons and at the ecosystem scale but also by assessing species-specific responses to eCO_2 in relation to trait expression. Amazon-wide expression of plant functional strategies may then be inferred by applying the mechanistic interplay between trait expression and edaphic conditions. The key to predicting the future of the world's largest tropical forest under eCO_2 thus lies in obtaining experimental data on, and subsequently modelling, different plant P acquisition and use strategies, as well as their interactions in a competing plant community.

END NOTES

Author contributions

D.M.L., A.R., and K.F. conceived the study. L.F., S.G., A.G., F.H., R.N., C.A.Q., K.J.S., and O.J.V.-B. collected field data. K.F., D.G., M. de K., M.J., V.H., J.H., F.L., L.M.M., B.P., C.v.R., Y.-P.W., X.Y., S.Z., and Q.Z. performed model simulations. K.F. wrote the manuscript with contributions from all co-authors.

Acknowledgements

We thank the many scientists involved in the development of the models used in our study; the many scientists, field and laboratory technicians and other staff involved in collecting and analysing the field data; and everyone involved in the planning and conductance of the AmazonFACE project. We thank the DFG for financing the workshop that made this study possible (grant No. RA 2060/4-1) and for providing funds to K.F. (grant No. RA 2060/5-1.)

REFERENCES

1. Brienen, R. J. W. *et al.* Long-term decline of the Amazon carbon sink. *Nature* **519,** 344–348 (2015).
2. Phillips, O. L. & Brienen, R. J. W. Carbon uptake by mature Amazon forests has mitigated Amazon nations' carbon emissions. *Carbon Balance Manag.* **12,** 1 (2017).
3. Cernusak, L. A. *et al.* Tropical forest responses to increasing atmospheric CO2: Current knowledge and opportunities for future research. *Funct. Plant Biol.* **40,** 531–551 (2013).
4. Huntingford, C. *et al.* Simulated resilience of tropical rainforests to CO$_2$-induced climate change. *Nat. Geosci.* **6,** 268–273 (2013).
5. Cox, P. M. *et al.* Sensitivity of tropical carbon to climate change constrained by carbon dioxide variability. *Nature* **494,** 341–344 (2013).
6. Ciais, P. *et al.* The physical science basis. Contribution of working group I to the fifth assessment report of the intergovernmental panel on climate change. *Chang. IPCC Clim.* 465–570 (2013). doi:10.1017/CBO9781107415324.015

7. Hofhansl, F. *et al.* Amazon forest ecosystem responses to elevated atmospheric CO2 and alterations in nutrient availability: filling the gaps with model-experiment integration. *Front. Earth Sci.* **4,** (2016).

8. Norby, R. J. *et al.* Model-data synthesis for the next generation of forest free-air CO2 enrichment (FACE) experiments. *New Phytol.* **209,** 17–28 (2016).

9. Talhelm, A. F. *et al.* Elevated carbon dioxide and ozone alter productivity and ecosystem carbon content in northern temperate forests. *Glob. Chang. Biol.* **20,** 2492–2504 (2014).

10. Norby, R. J., Warren, J. M., Iversen, C. M., Medlyn, B. E. & McMurtrie, R. E. CO2 enhancement of forest productivity constrained by limited nitrogen availability. *Proc. Natl. Acad. Sci.* **107,** 19368–19373 (2010).

11. Lloyd, J., Bird, M. I., Veenendaal, E. M. & Kruijt, B. Should Phosphorus Availability Be Constraining Moist Tropical Forest Responses to Increasing CO2 Concentrations? *Glob. Biogeochem. Cycles Clim. Syst.* 95–114 (2001). doi:10.1016/B978-012631260-7/50010-8

12. Vitousek, P. M. Litterfall, nutrient cycling, and nutrient limitation in tropical forests. *Ecology* **65,** 285–298 (1984).

13. Quesada, C. A. *et al.* Basin-wide variations in Amazon forest structure and function are mediated by both soils and climate. *Biogeosciences* **9,** 2203–2246 (2012).

14. Lambers, H., Raven, J. A., Shaver, G. R. & Smith, S. E. Plant nutrient-acquisition strategies change with soil age. *Trends Ecol. Evol.* **23,** 95–103 (2008).

15. Reed, S. C., Yang, X. & Thornton, P. E. Incorporating phosphorus cycling into global modeling efforts: A worthwhile, tractable endeavor. *New Phytol.* **208,** 324–329 (2015).

16. Turner, B. L., Brenes-Arguedas, T. & Condit, R. Pervasive phosphorus limitation of tree species but not communities in tropical forests. *Nature* **555,** 367–370 (2018).

17. Goll, D. S. *et al.* A representation of the phosphorus cycle for ORCHIDEE (revision 4520). *Geosci. Model Dev.* **10,** 3745–3770 (2017).

18. Wang, Y.-P., Law, R. M. & Pak, B. A global model of carbon, nitrogen and phosphorus cycles for the terrestrial biosphere. *Biogeosciences* **7,** 2261–2282 (2010).

19. Haverd, V. *et al.* A new version of the CABLE land surface model (Subversion

revision r4601) incorporating land use and land cover change, woody vegetation demography, and a novel optimisation-based approach to plant coordination of photosynthesis. *Geosci. Model Dev.* **11,** 2995–3026 (2018).

20. Comins, H. N. & McMurtrie, R. E. Long-Term Response of Nutrient-Limited Forests to CO"2 Enrichment; Equilibrium Behavior of Plant-Soil Models. *Ecol. Appl.* **3,** 666–681 (1993).

21. Zhu, Q., Riley, W. J., Tang, J. & Koven, C. D. Multiple soil nutrient competition between plants, microbes, and mineral surfaces: model development, parameterization, and example applications in several tropical forests. *Biogeosciences* **13,** 341–363 (2016).

22. Yang, X., Thornton, P. E., Ricciuto, D. M. & Post, W. M. The role of phosphorus dynamics in tropical forests – a modeling study using CLM-CNP. *Biogeosciences* **11,** 1667–1681 (2014).

23. Malhi, Y. *et al.* Comprehensive assessment of carbon productivity, allocation and storage in three Amazonian forests. *Glob. Chang. Biol.* **15,** 1255–1274 (2009).

24. Araújo, A. C. *et al.* Comparative measurements of carbon dioxide fluxes from two nearby towers in a central Amazonian rainforest: The Manaus LBA site. *J. Geophys. Res.* **107,** 8090 (2002).

25. Quesada, C. A. *et al.* Soils of Amazonia with particular reference to the RAINFOR sites. *Biogeosciences* **8,** 1415–1440 (2011).

26. Friend, A. D. *et al.* Carbon residence time dominates uncertainty in terrestrial vegetation responses to future climate and atmospheric CO $_2$. *Proc. Natl. Acad. Sci.* **111,** 3280–3285 (2014).

27. Walker, A. P. *et al.* Predicting long-term carbon sequestration in response to CO2 enrichment: How and why do current ecosystem models differ? *Global Biogeochem. Cycles* **29,** 476–495 (2015).

28. Vitousek, P. M. *Nutrient cycling and limitation: Hawai'i as a model system*. *Princeton University Press* (2004). doi:10.1016/j.dcn.2013.12.006

29. Nardoto, G. B. *et al.* Basin-wide variations in Amazon forest nitrogen-cycling characteristics as inferred from plant and soil 15N:14N measurements. *Plant Ecol. Divers.* **7,** 173–187 (2014).

30. Fyllas, N. M. *et al.* Basin-wide variations in foliar properties of Amazonian forest: phylogeny, soils and climate. *Biogeosciences* **6,** 2677–2708 (2009).

31. Wieder, W. R., Cleveland, C. C., Smith, W. K. & Todd-Brown, K. Future productivity and carbon storage limited by terrestrial nutrient availability. *Nat. Geosci.* **8,** 441–444 (2015).

32. Medlyn, B. E. *et al.* Using models to guide field experiments: a priori predictions for the CO2 response of a nutrient- and water-limited native Eucalypt woodland. *Glob. Chang. Biol.* **22,** 2834–2851 (2016).

33. Ellsworth, D. S. *et al.* Elevated CO2 does not increase eucalypt forest productivity on a low-phosphorus soil. *Nat. Clim. Chang.* **7,** 279–282 (2017).

34. Wright, S. J. *et al.* Plant responses to fertilization experiments in lowland, species-rich, tropical forests. *Ecology* **99,** 1129–1138 (2018).

35. Warren, J. M. *et al.* Root structural and functional dynamics in terrestrial biosphere models--evaluation and recommendations. *New Phytol.* **205,** 59–78 (2015).

36. Hoosbeek, M. R. Elevated CO2 increased phosphorous loss from decomposing litter and soil organic matter at two FACE experiments with trees. *Biogeochemistry* **127,** 89–97 (2016).

37. Yang, X., Thornton, P. E., Ricciuto, D. M. & Hoffman, F. M. Phosphorus feedbacks constraining tropical ecosystem responses to changes in atmospheric CO2 and climate. *Geophys. Res. Lett. Res.* 7205–7214 (2016). doi:10.1002/2016GL069241.Received

38. Vicca, S. *et al.* Fertile forests produce biomass more efficiently. *Ecol. Lett.* **15,** 520–526 (2012).

39. Gatti, L. V. *et al.* Drought sensitivity of Amazonian carbon balance revealed by atmospheric measurements. *Nature* **506,** (2014).

40. Powell, T. L. *et al.* Confronting model predictions of carbon fluxes with measurements of Amazon forests subjected to experimental drought. *New Phytol.* **200,** 350–365 (2013).

41. He, M. & Dijkstra, F. A. Drought effect on plant nitrogen and phosphorus: A meta-analysis. *New Phytol.* **204,** 924–931 (2014).

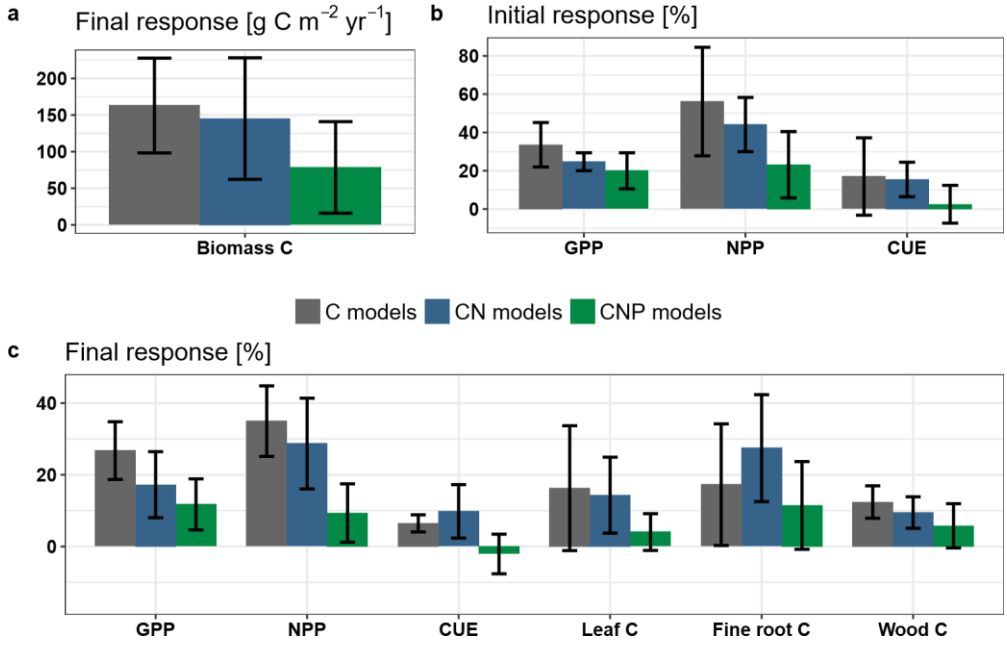

Figure 1: **The predicted effect of eCO_2 on biomass C, productivity and biomass compartments**, averaged over C (grey), CN (blue) and CNP (green) model groups. **a**, The final absolute response of biomass growth, calculated as the mean annual response over the 15 years of eCO_2 per model group in g C m^{-2} yr^{-1}. **b**, Initial relative responses of productivity (GPP and NPP), and CUE (=NPP/GPP) in %, calculated as the mean response in the first year. **c**, Final relative responses of productivity and CUE, as well as total leaf, fine root and wood C, calculated as the mean response after 15 years (mean of 13th to 17th year), all in %. Responses to eCO_2 are the differences between the elevated and ambient model run, shown as mean and standard deviation per model group, individual model outputs are shown in Extended Data Figure 1 and 3.

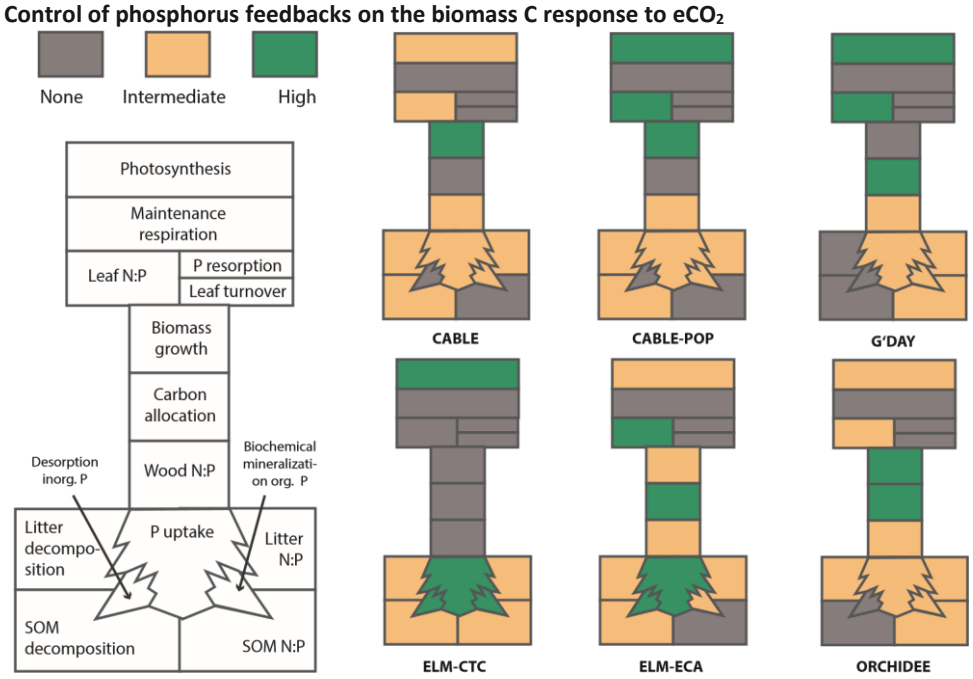

Figure 2: **Strength of phosphorus feedbacks in controlling the biomass C response to eCO_2 for the six CNP models.** Ecosystem processes are highlighted that depend (or not depend) on the P cycle, for which classes (none, intermediate, high) indicate the degree to which the considered P feedback causes a response of biomass C to eCO_2 in our simulations. P limitation causes strong or intermediate downregulation of photosynthesis with eCO_2 across all models. Maintenance respiration, leaf turnover and P resorption are not responsive to P feedbacks in any of the models. Leaf N:P responds to eCO_2 in most models, but is fixed in ELM-CTC, narrowly bound in CABLE, and at its maximum in ORCHIDEE. P limitation causes direct downregulation of biomass growth in CABLE, CABLE-POP, ELM-ECA and ORCHIDEE. Allocation shifts towards roots to alleviate P limitation is considered in GDAY, ELM-ECA and ORCHIDEE. Desorption of P from mineral surfaces is only considered in ELM-ECA and ELM-CTC, and biochemical P mineralization is considered in many models, but only effectively responsive in ELM-CTC.

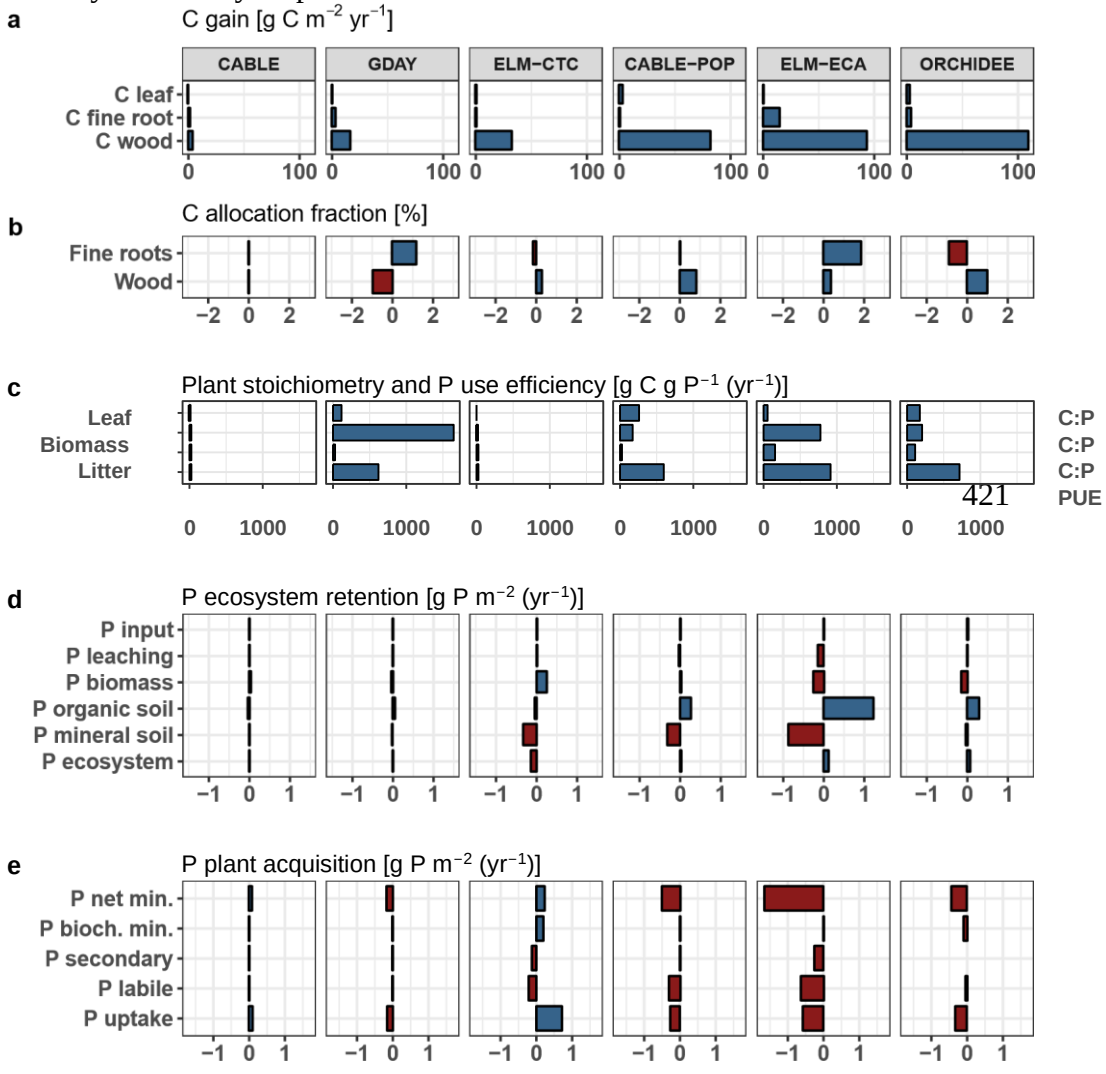

Figure 3: **Key responses of biomass C gain, stoichiometry, allocation, and P dynamics to eCO_2 for the CNP models**, contrasted are positive (blue) from negative (red) responses. **a**, Mean annual change in standing leaf, fine root and wood C over 15 years, increasing across models from left to right in g C m^{-2} yr^{-1}. **b**, The mean change in C allocation for fine roots and wood in %. **c**, Mean change in tissue stoichiometry in absolute terms in g C g P^{-1} and change in P use efficiency over 15 years in g C g P^{-1} yr^{-1}. **d**, Mean change in

ecosystem P input and output (leaching) fluxes in g P m^{-2} yr^{-1} and mean change in final P stock in biomass, organic soil, mineral soil and total ecosystem in g P m^{-2}. **e**, Mean change in plant P acquisition processes, including change in net P mineralization, biochemical P mineralization and P uptake in g P m^{-2} yr^{-1} and secondary and labile P pools in g P m^{-2}. For both, **d** and **e**, P flux changes are differences of cumulative fluxes after 15 years and P pool changes are differences in pools after 15 years.

CO_2 fertilization of the Amazon forest hinges on plant phosphorus use and acquisition

We present here supplementary information to the main text of the study "CO_2 fertilization of the Amazon forest hinges on plant phosphorus use and acquisition" by Fleischer et al., submitted to Nature Geoscience.

The individual models' biomass C responses to eCO_2 are shown in **Extended Data Figure 1**, where the absolute and relative effect of eCO_2 on cumulative biomass C is included. The variation in their predictions among and within the model groups becomes apparent. While CNP models (in green) generally predict lower biomass C gain with eCO_2 compared to Conly (grey) and CN models (blue), some CNP models exceed predictions by the other model groups. Assumptions on how plant P use and P acquisition is dealt with in the models cause these diverging responses.

The individual models' performance in representing ambient conditions of key ecosystem variables are shown in **Extended Data Figure 2**. Models' generally represented ambient conditions well at the study site, such as GPP, NPP and LAI. GPP was lower than observed in some models, while LAI was either over- or underestimated by some models. Considering the uncertainties surrounding field observations, we judged these deviations as acceptable. For biomass C, models diverged noticeably, which is controlled by productivity and turnover dynamics simultaneously. While we have relatively reliable measurements of aboveground biomass C, belowground components remain more uncertain and are not considered in the observational-based estimate here. Models on the other hand consider total biomass C, which adds to the differences among models and observations. Ambient annual biomass C increment varied strongly across the models, for which we included the Amazon-wide estimate from Brienen et al. 2015 as an observation (see main text for complete reference). The estimate from our site is lower (see main text), but associated to higher uncertainties due to few censuses. For both, biomass C and biomass C increment, there was no clear pattern between the model groups, so that we judge that these differences did not control the overall conclusions of our study.

The models simulated less than 1.1 g labile P m^{-2} to 4 m depth in the ambient run (with the exception of ELM-CTC), which is the plant available soil P. Observations indicate 1.6 g resin P m^{-2} to 30 cm depth. Resin P is considered to be directly plant-available, representing the modelled soil labile P pool, although direct comparisons are hampered as P fractionations are operationally defined. Observations are thus slightly higher but both modelled and observed values on soil labile P are considered to be very low and the resulting modelled P limitation to be realistic.

The individuals models' simulation results on the relative eCO_2 effect on primary productivity (GPP, NPP), plant tissue C stocks and plant CUE are shown in **Extended Data Figure 3**. The models' plant C allocation fractions and the respective relative effect of eCO_2 thereon is shown in **Extended Data Figure 4**. The individuals models' simulation results on

the relative eCO_2 effect on N and P uptake, NUE and PUE, as well as plant tissue stoichiometry is shown in **Extended Data Figure 5**.

The relationship between eCO_2 induced P uptake, fine root allocation, and the respective return of P uptake per unit fine root allocation for three CNP models are shown in **Extended Data Figure 6**. The three models (ELM-ECA, GDAY, and ORCHIDEE) simulated a higher fine root investment with eCO_2, but a heightened relative return of P was only achieved temporarily, after some time, or not at all. The absolute effect of eCO_2 on NUE, PUE and stoichiometry for the individual models is shown in **Extended Data Figure 7**. Both CN and CNP versions of GDAY and CABLE-POP were included in the model ensemble, allowing the N and P effect alone to be inferred. Their respective CN versions, and some other CN models, indicated that N limitation occurred, as leaf and biomass C:N were predicted to increase under eCO2 (Extended Data Fig. 7). The inclusion of both CN and CNP versions for GDAY and CABLE-POP supported the fact that P cycle limitations reduced the eCO_2 induced biomass C sink, as the main comparison across the C, CN and CNP model group indicated.

Model driving data of precipitation are plotted as annual precipitation over the course of the 15 year study period in **Extended Data Figure 8**. Precipitation (and other climate) data was derived from the K34 fluxtower, which experienced two years of strong precipitation deficit during the study period, 2000 and 2009. The relative eCO_2 response of GPP and NPP is plotted against annual precipitation in the **Extended Data Figure 9** to test for potential interactions of eCO_2 and droughts in the study region. While some models show a significant effect of precipitation on the strength of the eCO_2 effect on GPP, the slope of the line is very shallow, so that we can conclude that variations in water availability contributed little to the simulated eCO_2 effect in our study.

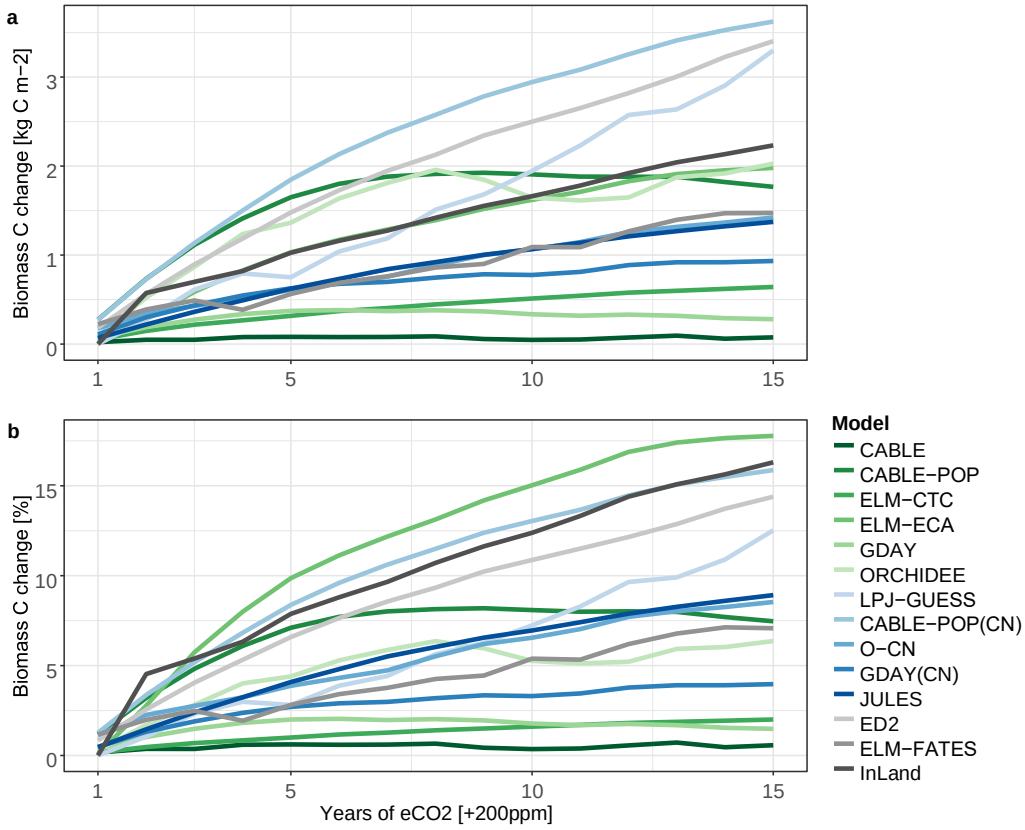

Extended Data Figure 1: **Cumulative effect of eCO_2 on biomass C per model. a**, Absolute cumulative effect on biomass C in kg C m^{-2}, and **b**, relative cumulative effect on

biomass C in %. See legend for individual model names. C-only models are in shades of grey, CN models are depicted in shades of blue and CNP models are depicted in shades of green.

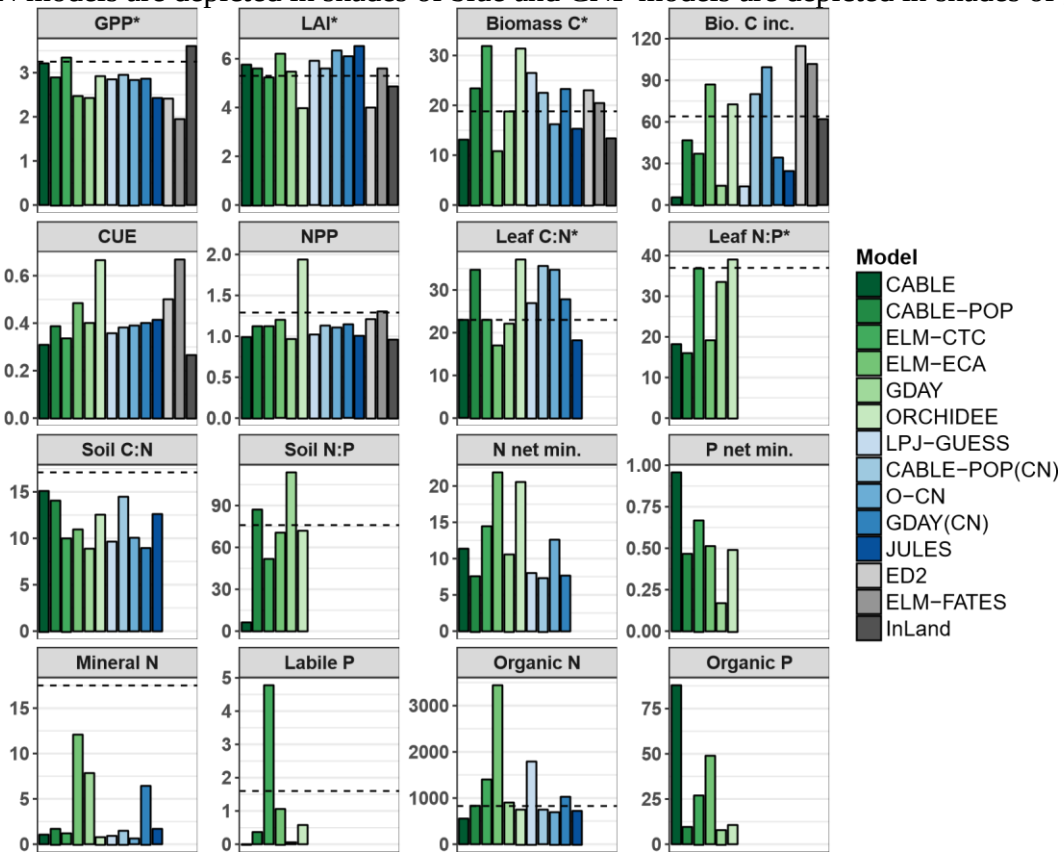

Extended Data Figure 2: **Ambient model conditions compared to** *in situ* **observations.** Individual models' values are mean conditions over the ambient simulation. Horizontal dotted lines indicate observations when available (see sources in Extended Data Table 1). Measurements marked with a *?* were provided to modelers beforehand. C fluxes (GPP, NPP) are in kg C m^{-2} yr^{-1}, biomass C is aboveground only in kg C m^{-2}, and biomass C increment in g C m^{-2} yr^{-1}. The observational estimate for biomass C increment is based on the Amazon-wide estimate from Brienen et al. 2015 (64 g C m^{-2} yr^{-1} for the 2000s, C.I. 45-78 g C m^{-2} yr^{-1}). CUE is calculated as the ratio of NPP per GPP. LAI is in m^2/m^2. Leaf and soil stoichiometry are ratios of C, N and P content in dry matter, respectively. Leaf stoichiometry was parameterised only in some models (see Extended Data Table 2). Fluxes of net N and P mineralisation are in g N/P m^{-2} yr^{-1}. Soil mineral N pool and labile P pool (both considered plant-available), as well as soil organic N and P pool, are in g N/P m^{-2}. Observations for soil nitrogen content are based on top 10 cm, and for labile P on top 30cm. Modeled values are based on a soil depth of 4m. See legend for individual model names. C-only models are in shades of grey, CN models are depicted in shades of blue and CNP models are depicted in shades of green.

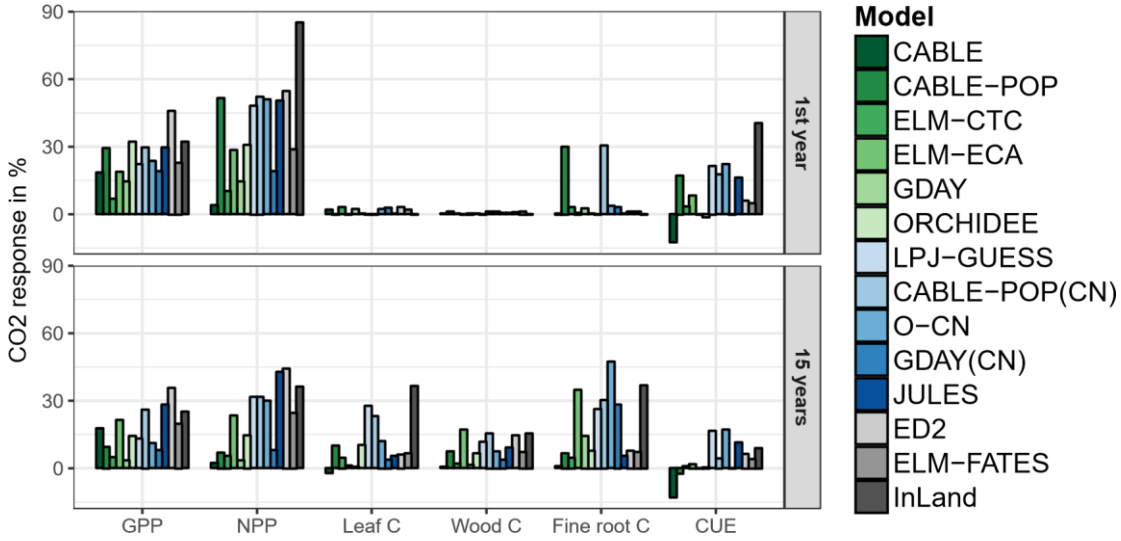

Extended Data Figure 3: **Relative effect of eCO_2 on GPP, NPP, leaf C, wood C, fine root C and plant CUE.** Shown are initial effects (1st year) on top and final effect after 15 years of eCO_2 (mean of 13th to 17th year), both in %. See legend for individual model names. C-only models are in shades of grey, CN models are depicted in shades of blue and CNP models are depicted in shades of green.

Extended Data Figure 4: **Ambient C allocation to plant tissues and the effect of eCO_2 thereon.** Mean and standard deviation of ambient C allocation to leaf, wood, coarse and fine

root per model in % (top), and annual effect of eCO_2 on C allocation fractions over 15 years per model in % (bottom). See legend for tissue compartments; leaf is displayed in green, wood in red, coarse root in dark blue and fine root in light blue. Note individual y-axis scaling in bottom graph.

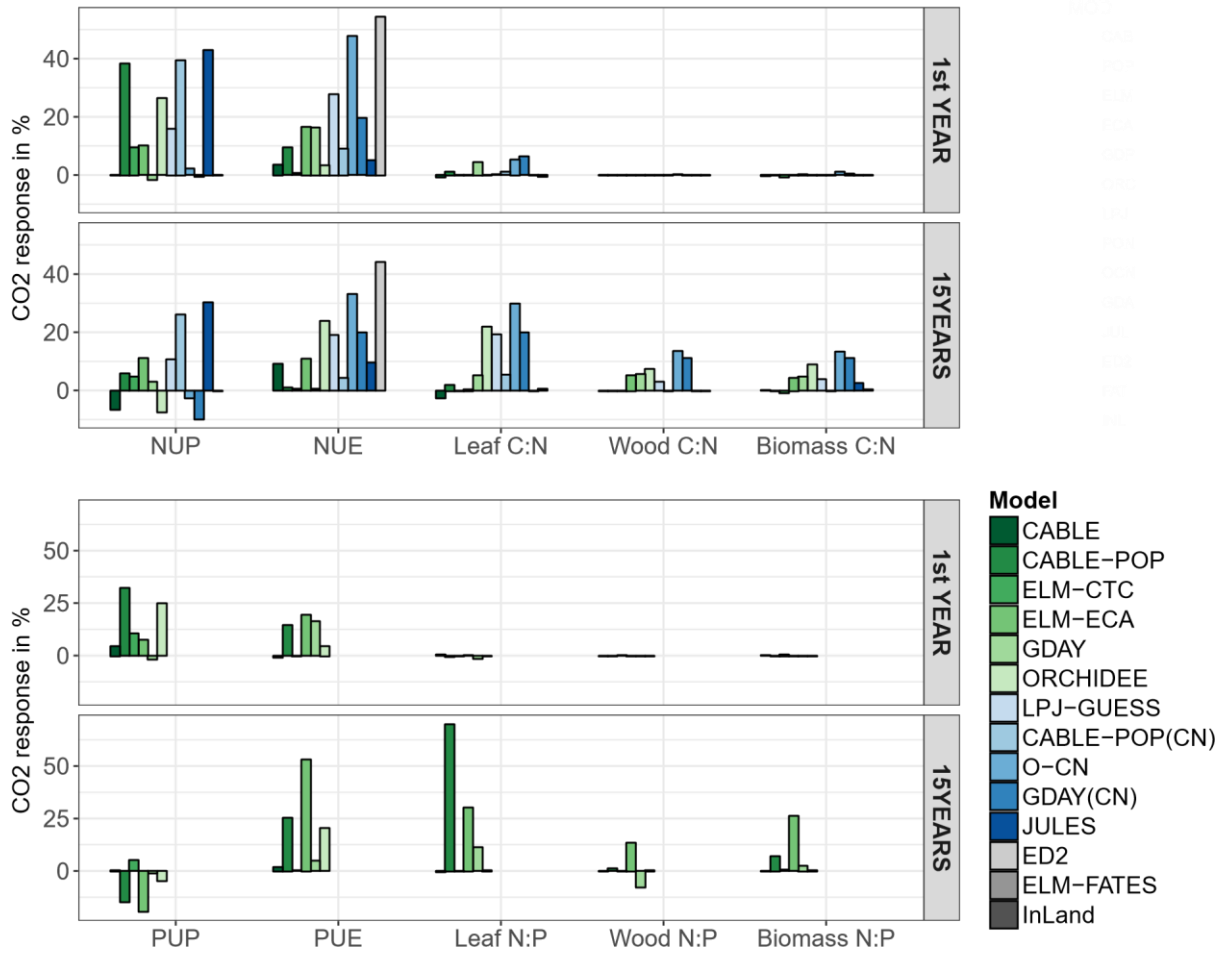

Extended Data Figure 5: **Relative effect of eCO_2 on N and P uptake, NUE and PUE, and biomass stoichiometry per model.** Shown are initial effects (1st year), and final effects after 15 years of fumigation (mean of 13th to 17th year), for N uptake (NUP), N use efficiency (NUE), leaf C:N, Wood C:N, and biomass C:N for all CN and CNP models, in % (top). Further displayed are P uptake (PUP), P use efficiency (PUE), leaf N:P, wood N:P, and biomass N:P for all CNP models, in % (bottom). See legend for individual model names. C-only models are in shades of grey, CN models are depicted in shades of blue and CNP models are depicted in shades of green.

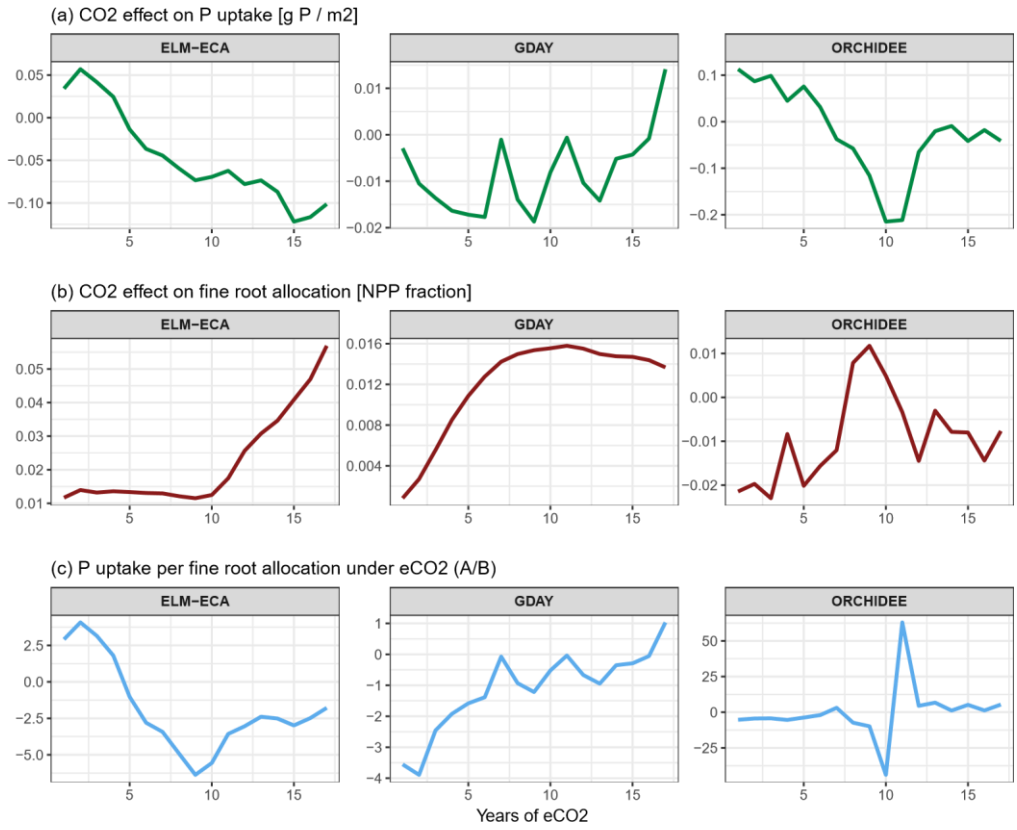

Extended Data Figure 6: **Effect of CO_2 on P uptake, fine root investment and the resulting P uptake per fine root investment. a**, CO_2 effect on P uptake, **b**, CO_2 effect on fine root allocation, and **c**, P uptake gain per fine root investment (a/b). Shown for the three CNP models that predict higher fine root investment with eCO_2, see plot title for individual model names.

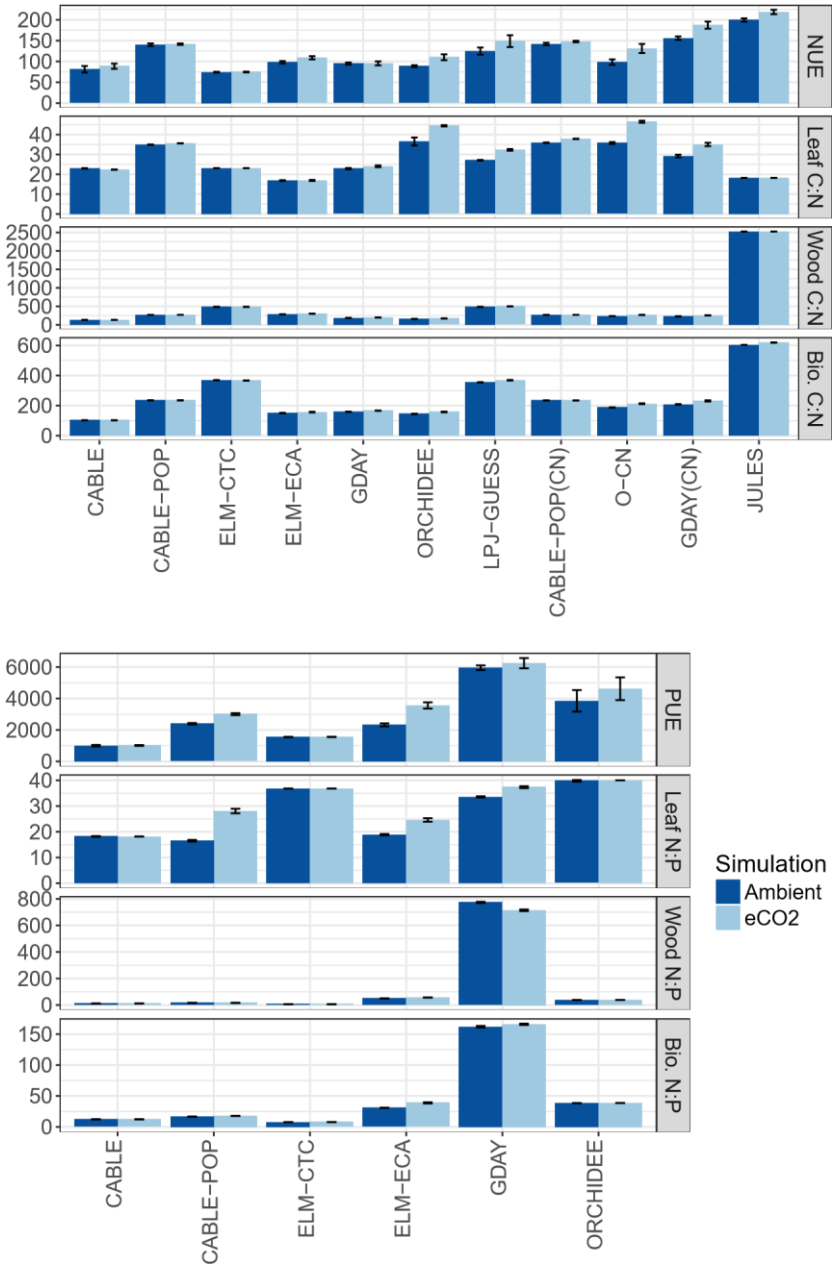

551

552 **Extended Data Figure** 7: **Absolut CO_2 effect on nutrient use efficiency and biomass**
553 **stoichiometry per model.** Shown are the absolut difference between ambient and eCO_2
554 simulation run at the end of the 15 year simulation experiment (mean and standard deviation
555 of 13th to 17th year) for nitrogen use efficiency (NUE), leaf C:N, wood C:N, and plant
556 biomass C:N for CN and CNP models (top), and for phosphorus use efficiency (PUE), leaf
557 N:P, wood N:P, and plant biomass N:P for CNP models (bottom). See x-axis for individual
558 model names.

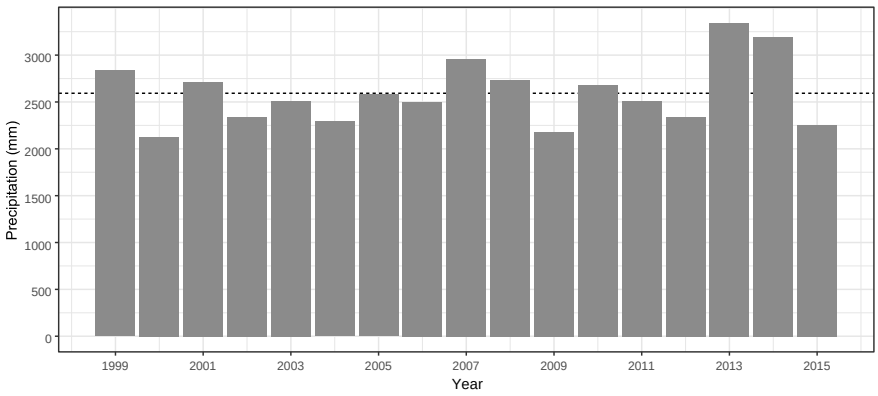

559

560 **Extended Data Figure** 8: **Annual precipitation from the fluxtower K34, used as**
561 **model driving data.** Shown are sums of annual precipitation in mm, note that years
562 represent Southern hemisphere growing season, i.e. 01/07/year to 30/06/year+1.

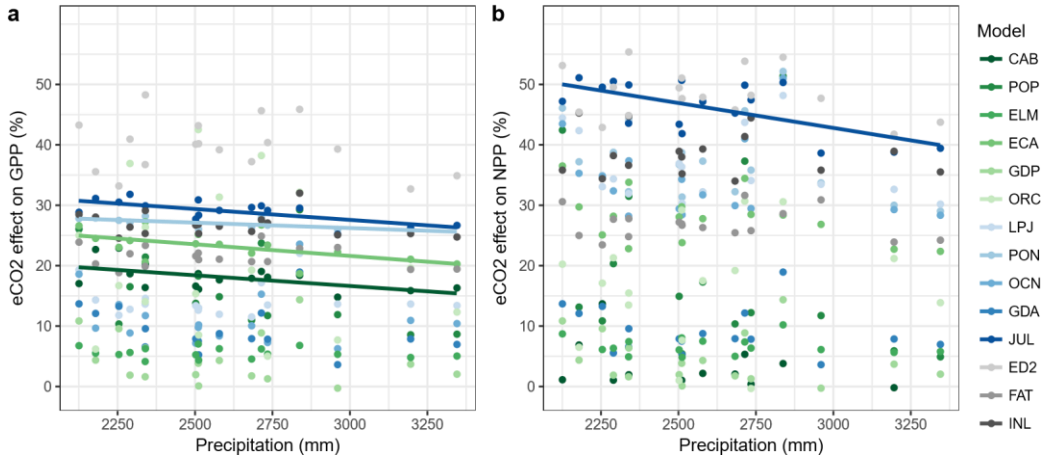

563

564 **Extended Data Figure** 9: **Effect of precipitation on the individual models' eCO2**
565 **effect on GPP and NPP. a**, eCO2 effect on gross primary production (GPP) (in %) and **b**,
566 eCO2 effect on net primary production (NPP), both against sum of precipitation (in mm)
567 throughout the experimental phase (1999-2015). See legend for individual model names. C-
568 only models are in shades of grey, CN models are depicted in shades of blue and CNP models
569 are depicted in shades of green. Only significant (p¡0.05) linear regression lines are drawn in
570 the respective colour per model.
571